Journal of Sound and Vibration (2002) **254**(2), 367–378
doi:10.1006/jsvi.5004, available online at http://www.idealibrary.com on IDEAL®

VIBRATION ANALYSIS OF A DAMPED ARCH USING AN ITERATIVE LAMINATE MODEL

B. KOVÁCS

Institute of Mathematics, University of Miskolc, 3515 *Miskolc-Egyetemváros, Hungary*

(*Received* 10 *April* 2001, *and in final form* 28 *September* 2001)

A new model is presented for the dynamic analysis of a laminated circular ring segment. The differential equations which govern the free vibrations of a circular ring segment and the associated boundary conditions are derived by Hamilton's principle having consideration for the bending and shear deformation of all layers. The author uses a new iterative process to successively refine the stress/strain field in the sandwich arch. The model includes the effects of transverse shear and rotatory inertia. The iterative model is used to predict the modal frequencies and damping of simply-supported sandwich circular arch. The solutions for a three-layer circular arch are compared with a three-layer approximate model.

1. INTRODUCTION

Laminated composite curved beams have been used in engineering applications for many years. Design applications of isotropic and curved bars, rings and arches of arbitrary shape are assisted by a well-developed theory and proven design guidelines [1–4]. The development of the theory and design guidelines for composite curved beams is much less satisfactory. Earlier works relate to sandwich beams or closed composite rings [5–9]. The finite element method was used to study the dynamic response of sandwich curved beams by Ahmed [5, 6]. Free and forced vibrations of a three-layer damped ring were investigated by Di Taranto [7]. Lu and Douglas [8] investigated the damped three-layered sandwich ring subjected to a time harmonic radially concentrated load. The paper gives an analytical solution for the mechanical impedance at an arbitrary point on the surface of the damped structure as a function of the forcing frequency. Furthermore, an experimental procedure is employed to measure the driving point mechanical impedance as a verification of the calculated results. Transient response was studied for three-layer closed rings by Sagartz [9]. Damping properties of curved sandwich beams with viscoelastic layer were studied by Tatemichi *et al.* [10]. Viscoelastic damping in the middle core layer was emphasized.

Nelson and Sullivan [11] analyzed the complete circular ring consisting of a layer soft viscoelastic material sandwiched between two hard elastic layers. The equations which govern the forced vibration of a damped circular ring were solved by the method of damped forced modes. The essence of the damped forced mode method is the use of harmonic forcing functions which are in-phase with the local velocity and proportional to the local inertia loads. The constant of proportionality is the loss factor of the composite structure, η_n. A clear alternative to a damped forced mode solution is to set all the forcing functions to zero and solve the resulting complex eigenvalue problem. Isvan and Nelson [12] have investigated the natural frequencies and composite loss factors of the free vibration of

0022-460X/02/$35.00

a soft-cored circular arch simply supported at each end. Although harmonic motion is assumed, what is not stated is that some harmonic excitation is required to maintain such motion in the presence of damping. The dynamic eigenvalue problem is then posed for an unforced system. Kovacs [13] solved the problem of free vibrations of a stiff-cored sandwich circular arch. All the tangential displacement components are assumed to be piecewise linear across the thickness, thus implying the inclusion of shear deformations and rotary inertia.

The incremental equations of motion based on the principle of virtual displacements of a continuous medium are formulated using the total Lagrangian description by Liao and Reddy [14]. They developed a degenerate shell element with a degenerate curved beam element as a stiffener for the geometric non-linear analysis of laminated, anisotropic, stiffened shells. Bhimaraddi *et al.* [15] presented a 24 d.o.f. of isoparametric finite element for the analysis of generally laminated curved beams. The rotary inertia and shear deformation effects were considered in this study. Qatu developed a consistent set of equations for laminated shallow [16] and with Elsharkawy for deep arches [17]. Exact solutions are presented for laminated arches having general boundary conditions by Qatu [18]. The in-plane free vibrational analysis of symmetric cross-ply laminated circular arches was studied by Yildirim [19]. The derivation of the free vibration equations are based on the distributed parameter model. The transfer matrix method is used in the analysis. The rotary inertia, axial and shear deformation effects are considered in the Timoshenko analysis by first order shear deformation theory. Vaswani *et al.* [20] have derived by the Ritz method a closed-form solution for the system loss factors and resonance frequencies for a curved sandwich beam with a viscoelastic core. He and Rao [21] have used the energy method and Hamilton's principle to derive the governing equation of motion for the coupled flexural and longitudinal vibration of a curved sandwich beam system. Both shear and thickness deformations of the adhesive core are included. Equations for obtaining the system modal loss factors and resonance frequencies were derived for a system having simply-supported ends by the Ritz method.

It is well known that the accurate determination of the stress field in the laminate configurations is particularly important for "stress critical" calculations such as damping and delamination. Zapfe and Lesieutre [22] developed an iterative process to refine successively the shape of the stress/strain distribution for the dynamic analysis of laminated beams. The iterative model is used to predict the modal frequencies and damping of simply supported beams with integral viscoelastic layers.

The eigenproblem of the plane bending of circular arch-shaped layered beams was investigated by using the finite element method by Kovacs *et al.* [23]. The finite element model of the structure has two elements along the face thickness and three elements along the thickness of the core. The two edges of the circular arch are simply supported. This model consists of eight-node hexahedron 3D elements (280 pcs).

Flexure of the three-layer sandwich arch results in energy dissipation due to strains induced in the viscoelastic layer. In a symmetrical arrangement with identical elastic layers, most of the damping is due to shear in the viscoelastic layer. In an unsymmetrical arrangement, with dissimilar elastic layers, one might expect damping due to direct strain as well as shear in the viscoelastic layer, the former being known as extensional damping and the latter as shear damping. Both these effects have been included by Kovacs [24]. However, the stress–strain law assumed for the viscoelastic layer was not strictly correct and was only an approximation if extensional effects were considered. An analysis of the vibration of transversely isotropic beams, which have small constant initial curvature was presented by Rossettos [25], and Rossettos and Squires [26]. A closed-form general solution to the governing equations was derived. Natural modes and frequencies were

determined for both clamped and simply-supported end conditions. In reference [27], an analysis of the vibration of slightly curved cross-ply laminated composite beams is presented. Hamilton's principle is used to derive the equations of motions of four theories. Exact natural frequencies are determined for various end conditions using the state-space concept. The combined effects of initial curvature, transverse shear deformation, orthotropicity ratio, stacking sequence and boundary conditions are evaluated and discussed. Yildirim [28] offers a comprehensive analysis of free vibration characteristics of symmetric cross-ply laminated circular arches vibrating perpendicular to their planes. Governing equations of symmetric laminated circular arches made of a linear, homogeneous, and orthotropic material are obtained in a straightforward manner based on the classical beam theory. The transfer matrix method is used for the free vibration analysis of the continuous parameter system.

The present research extends the iterative laminated model developed by Zapfe and Lesieutre to the dynamic analysis of laminated circular ring segment. The current model is developed for the specific case of simply-supported circular ring segment with uniform properties along the length.

2. GOVERNING EQUATIONS OF MOTION

The geometry of interest and the notation used are shown in Figure 1. As indicated in the figure, the ring segment ends are simply supported. Consider the curved sandwich arch with a circular centreline and a constant rectangular cross-section. The arch consists of three different layers of homogeneous materials bonded together to form a composite arch. Subscript i, where $i = 1, 2, 3$ is used to denote quantities in the various layers, starting from the outermost layer, so that layers 1, 3 represent the elastic layers while 2 represents the viscoelastic layer. A state of plane stress is assumed, as well as the fact that the materials in each layer of the arch are homogeneous isotropic. Perfect bonding of the layers and linear elasticity are also assumed in the analysis. The composite arch is lightly damped and it is assumed that all the energy is dissipated in the viscoelastic layer. The radial displacement is

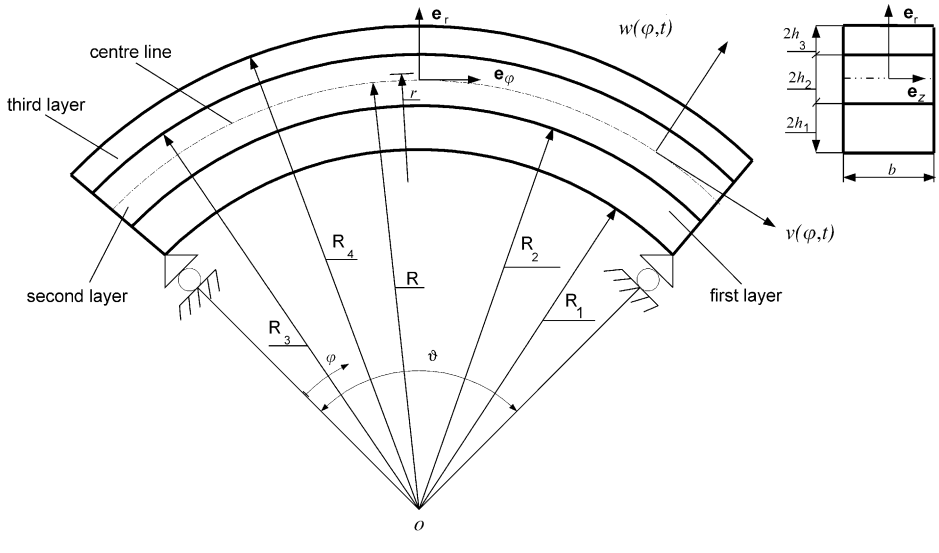

Figure 1. The geometry of the laminated circular ring segment.

the same for all three layers. The form of the displacement field over the domain of the circular arch is

$$\mathbf{t}(r, \varphi, t) = u(r, \varphi, t)\mathbf{e}_\varphi + w(\varphi, t)\mathbf{e}_r$$
$$= \left[v(\varphi, t) - \frac{r - R}{R}\left(\frac{\partial w}{\partial \varphi} - v(\varphi,t)\right) + f(r)g(\varphi, t) \right]\mathbf{e}_\varphi + w(\varphi, t)\mathbf{e}_r, \tag{2.1}$$

where $f(R) = 0$.

The term $f(r)g(\varphi, t)$ can be considered as a correction to account for transverse shear effects. The function $f(r)$ represents the shape of the correction through the thickness of the arch, while $g(\varphi, t)$ determines its distribution along the length. The solution of a given problem requires the determination of the unknown functions $v(\varphi, t)$, $w(\varphi, t)$, $g(\varphi, t)$ and $f(r)$.

By using

$$\mathbf{t} = w\mathbf{e}_r + u\mathbf{e}_\varphi, \quad \varepsilon_\varphi = \frac{1}{r}\frac{\partial u}{\partial \varphi} + \frac{w}{r}, \quad \gamma_{r\varphi} = \frac{1}{r}\frac{\partial w}{\partial \varphi} + \frac{\partial u}{\partial r} - \frac{u}{r}$$

standard expressions the strain tensor of each layer can be computed from equations (2.1)

$$\varepsilon_\varphi = \frac{1}{r}\left[\frac{\partial v}{\partial \varphi} - \frac{r - R}{R}\left(\frac{\partial^2 w}{\partial \varphi^2} - \frac{\partial v}{\partial \varphi}\right) + f(r)\frac{\partial g}{\partial \varphi} + w\right], \tag{2.2}$$

$$\gamma_{r\varphi} = \left[\frac{\mathrm{d}f}{\mathrm{d}r} - \frac{f}{r}\right]g(\varphi, t). \tag{2.3}$$

From equation (2.3), it can be seen that the function $\mathrm{d}f/\mathrm{d}r - f/r$ represents the shape of the transverse shear strain field through the thickness of the arch, at a given φ-location. While the assumed form of the shear correction, $f(r)$ will change from one iteration to the next, at any given iteration it can be treated as a known function.

The strain energy stored in the circular arch is given by

$$U = \frac{b}{2}\sum_{i=1}^{3}\int_{\varphi=0}^{\vartheta}\int_{R_i}^{R_i+1}[E_i(\varepsilon_{\varphi i})^2 + G_i(\gamma_{r\varphi i})^2]r\,\mathrm{d}r\,\mathrm{d}\varphi. \tag{2.4}$$

The kinetic energy, which includes components associated with transverse, in plane and rotary inertia, is given by

$$T = \frac{b}{2}\sum_{i=1}^{3}\int_{\varphi=0}^{\vartheta}\int_{R_i}^{R_i+1}\rho_i(\dot{\mathbf{t}}_i)^2\,r\,\mathrm{d}r\,\mathrm{d}\varphi, \tag{2.5}$$

where the dots over $\mathbf{t}_1$, $\mathbf{t}_2$ and $\mathbf{t}_3$ denote the partial derivative with respect to time. The differential equations of motion and boundary conditions are derived using Hamilton's principle. The equations of motion for the three unknown functions, $w(\varphi, t)$, $v(\varphi, t)$ and $g(\varphi, t)$ are

$$A_{11}\frac{\partial^4 w}{\partial \varphi^4} + A_{12}\frac{\partial^2 w}{\partial \varphi^2} + A_{13}\frac{\partial^3 v}{\partial \varphi^3} + A_{14}\frac{\partial^3 g}{\partial \varphi^3} + A_{15}\frac{\partial v}{\partial \varphi} + A_{16}\frac{\partial g}{\partial \varphi} + A_{17}w$$
$$= D_{11}\frac{\partial^4 w}{\partial \varphi^2 \partial t^2} + D_{12}\frac{\partial^3 v}{\partial \varphi \partial t^2} + D_{13}\frac{\partial^3 g}{\partial \varphi \partial t^2} + D_{14}\frac{\partial^2 w}{\partial t^2}, \tag{2.6}$$

$$A_{21}\frac{\partial^3 w}{\partial\varphi^3} + A_{22}\frac{\partial w}{\partial\varphi} + A_{23}\frac{\partial^2 v}{\partial\varphi^2} + A_{24}\frac{\partial^2 g}{\partial\varphi^2} + A_{25}g$$

$$= D_{21}\frac{\partial^3 w}{\partial\varphi\partial t^2} + D_{22}\frac{\partial^2 v}{\partial t^2} + D_{23}\frac{\partial^2 g}{\partial t^2}, \tag{2.7}$$

$$A_{31}\frac{\partial^3 w}{\partial\varphi^3} + A_{32}\frac{\partial w}{\partial\varphi} + A_{33}\frac{\partial^2 v}{\partial\varphi^2} + A_{34}\frac{\partial^2 g}{\partial\varphi^2} = D_{31}\frac{\partial^3 w}{\partial\varphi\partial t^2} + D_{32}\frac{\partial^2 v}{\partial t^2} + D_{33}\frac{\partial^2 g}{\partial t^2}, \tag{2.8}$$

where A_{ij} and D_{ij} are given in Appendix A. $K_{1\text{-}7}$ and $M_{1\text{-}6}$ are section stiffness and mass coefficients, given by

$$K_{[1,2,3,4,5,6]} = b\sum_{i=1}^{3}\int_{R_i}^{R_i+1} E_i\left[1, r, f_i(r), \frac{1}{r}f_i(r), \frac{1}{r}, \frac{1}{r}f_i^2(r)\right]\mathrm{d}r, \tag{2.9}$$

$$K_{[7]} = b\sum_{i=1}^{3}\int_{R_i}^{R_i+1} G_i r\left[\frac{\mathrm{d}f_i}{\mathrm{d}r} - \frac{f_i}{r}\right]^2\mathrm{d}r, \tag{2.10}$$

$$K_{[1,2,3,4,5,6]} = b\sum_{i=1}^{3}\int_{R_i}^{R_i+1} \rho_i[r, r^2, r^3, rf_i(r), r^2 f_i(r), rf_i^2(r)]\mathrm{d}r, \tag{2.11}$$

where $f(r) = \begin{cases} f_1(r) & \text{if } R_1 \leqslant r \leqslant R_2, \\ f_2(r) & \text{if } R_2 \leqslant r \leqslant R_3, \\ f_3(r) & \text{if } R_3 \leqslant r \leqslant R_4 \end{cases}$

is a single-valued function defined at each point through the thickness.

The kinematic and natural boundary conditions specified at $\varphi = 0$ and ϑ, are given by

Kinematic		*Natural*
$v = 0$	or	$F_{11}\partial^2 w/\partial\varphi^2 + F_{12}\partial v/\partial\varphi + F_{13}\partial g/\partial\varphi = 0,$
$w = 0$	or	$F_{21}\partial^3 w/\partial\varphi^3 + F_{22}\partial^2 v/\partial\varphi^2 + F_{23}\partial^2 g/\partial\varphi^2 + F_{24}\partial^3 w/\partial\varphi^2\partial t + F_{25}\partial^2 v/\partial t^2 + F_{26}\partial^2 g/\partial t^2 = 0,$
$g = 0$	or	$F_{31}\partial^2 w/\partial\varphi^2 + F_{32}\partial v/\partial\varphi + F_{33}\partial g/\partial\varphi = 0,$
$\partial w/\partial\varphi = 0$	or	$F_{41}\partial^2 w/\partial\varphi^2 + F_{42}\partial v/\partial\varphi + F_{43}\partial g/\partial\varphi = 0,$

(2.12)

where F_{ij} are constants. For the special case of a simply-supported arch, the first, third and fourth natural boundary conditions are combined with the kinematic condition, $w = 0$.

3. SOLUTION FOR A SIMPLY SUPPORTED ARCH

Sinusoidal mode shapes that satisfy the boundary conditions are assumed. Consequently, the assumed displacements are

$$w(\varphi, t) = W\sin(k_n\varphi)\mathrm{e}^{\mathrm{i}\omega_n t}, \qquad v(\varphi, t) = V\cos(k_n\varphi)\mathrm{e}^{\mathrm{i}\omega_n t}, \qquad g(\varphi, t) = G\cos(k_n\varphi)\mathrm{e}^{i\omega_n t}, \tag{3.1–3.3}$$

where $k_n = (n\pi)/\vartheta$. Since the motion is now harmonic, it is legitimate to admit hysteretic damping into the viscoelastic layer by putting the moduli a complex form. Young's and the shear modulus of the constituent materials are represented by the complex quantities

$$\mathbf{E}_2^* = E_2(1 + \mathrm{i}\alpha_2), \qquad \mathbf{G}_2^* = G_2(1 + \mathrm{i}\beta_2), \tag{3.4}$$

where α_2 and β_2 denote the material loss factors in extension and shear respectively. Since the complex $\mathbf{G}_2^*$ and $\mathbf{E}_2^*$ are used as complex moduli of the middle layer, the differential equations of motion will have complex coefficients. The substitution of equations (3.1), (3.2) and (3.3) into equations (2.6), (2.7) and (2.8), will result in a set of three simultaneous, homogeneous algebraic equations with symmetric and complex coefficients. In matrix form, these equations are

$$[-\omega_n^2[\mathbf{M}] + [\mathbf{K}]]\{\mathbf{U}\} = 0, \qquad \{\mathbf{U}\} = \{\mathbf{V}, \mathbf{W}, \mathbf{G}\}, \tag{3.5}$$

where M_{ij} and K_{ij} are in Appendix A. The complex eigenvalues give the desired natural frequencies and mode shapes with their phase relations. The natural frequency is approximately equal to the square root of the real part of the eigenvalue. The modal loss factor for the nth mode is approximately equal to the ratio of the imaginary part of the eigenvalue to the real part of the eigenvalue

$$\eta_n = \mathrm{Im}(\omega_n^2)/Re(\omega_n^2). \tag{3.6}$$

4. IMPROVED ESTIMATE FOR SHEAR CORRECTION FUNCTION $f(r)$

An improved estimate for the shear correction function $f(r)$ is derived from the equation of elemental stress equilibrium. The equations of motion in plane stress

$$\frac{\partial}{\partial r}[r^2\tau_{r\varphi}] + r\frac{\partial \sigma_\varphi}{\partial \varphi} = r^2\rho\frac{\partial^2 u}{\partial t^2} \tag{4.1}$$

applied to the layered arch with $\sigma_{\varphi i} = E_i\,\varepsilon_{\varphi i}$ expressions, are now in the form

$$\frac{\partial}{\partial r}(r^2\tau_{r\varphi i}) + E_i\left[\frac{\partial^2 v}{\partial \varphi^2} - \frac{r-R}{R}\left(\frac{\partial^3 w}{\partial \varphi^3} - \frac{\partial^2 v}{\partial \varphi^2}\right) + f_i(r)\frac{\partial^2 g}{\partial \varphi^2} + \frac{\partial w}{\partial \varphi}\right]$$

$$= r^2\rho_i\left[\frac{\partial^2 v}{\partial t^2} - \frac{r-R}{R}\left(\frac{\partial^3 w}{\partial \varphi \partial t^2} - \frac{\partial^2 v}{\partial t^2}\right) + f_i(r)\frac{\partial^2 g}{\partial t^2}\right], \tag{4.2}$$

where $i = 1, 2, 3$ and $R_i \leqslant r \leqslant R_{i+1}$.

By virtue of equations (2.3), (3.1), (3.2) and (3.3), it is obvious that equation (4.2) can be written in the form

$$\frac{\partial}{\partial r}(r^2\mathring{\tau}_{r\varphi i}) + E_i\left[-k_n^2 V - \frac{r-R}{R}(-k_n^3 W + k_n{}^2 V) - f_i(r)k_n^2 G + k_n W\right]$$

$$= -r^2\rho_i\omega_n^2\left[V - \frac{r-R}{R}(k_n W - V) + f_i(r)G\right], \tag{4.3}$$

where $\tau_{r\varphi i}(r, \varphi, t) = \mathring{\tau}_{r\varphi i}(r)\cos(k_n\varphi)\mathrm{e}^{\mathrm{i}\omega_n t}$.

The shape of the shear stress distribution can be found by integrating equation (4.3) through the thickness

$$\overset{\circ}{\tau}_{r\varphi i}(r) = \frac{1}{r^2}\, c_i + \frac{1}{r^2}\int_{R_i}^{r} - E_i\Bigg[- k_n^2 V - \frac{r-R}{R}(- k_n^3 W + k_n^2 V) - f_i(r) k_n^2 G + k_n W \Bigg]$$

$$- r^2 \rho_i \omega_n^2 \Bigg[V - \frac{r-R}{R}(k_n W - V) + f_i(r)\, G \Bigg] \mathrm{d}r, \tag{4.4}$$

where

$$c_1 = 0, \quad c_2 = R_2^2 \overset{\circ}{\tau}_{r\varphi 1}(R_2), \quad c_2 = R_3^2 \overset{\circ}{\tau}_{r\varphi 2}(R_3). \tag{4.5}$$

The shape of the shear strain distribution is calculated using equation (4.4) and the constitutive relation

$$\gamma_{r\varphi i}(r) = \overset{\circ}{\tau}_{r\varphi i}(r)/G_i, \quad i = 1, 2, 3. \tag{4.6}$$

The new estimate for the shear correction function $f(r)$ obtained by integrating equation (2.3) through the thickness, is given by

$$f_1(r) = r\Bigg[\int_R^{R_2} \frac{1}{r}\, \gamma_{r\varphi 2}(r)\, \mathrm{d}r + \int_{R_2}^{r} \frac{1}{r}\, \gamma_{r\varphi 1}(r)\, \mathrm{d}r \Bigg], \quad R_1 \leqslant r \leqslant R_2, \tag{4.7}$$

$$f_2(r) = r\int_R^{r} \frac{1}{r}\, \gamma_{r\varphi 2}(r)\, \mathrm{d}r, \quad R_2 \leqslant r \leqslant R_3, \tag{4.8}$$

$$f_3(r) = r\Bigg[\int_R^{R_3} \frac{1}{r}\, \gamma_{r\varphi 2}(r)\, \mathrm{d}r + \int_{R_3}^{r} \frac{1}{r}\, \gamma_{r\varphi 3}(r)\, \mathrm{d}r \Bigg], \quad R_3 \leqslant r \leqslant R_4, \tag{4.9}$$

with evidently $f(R) = f_2(R) = 0$ at the reference axis. The integrals in equations (4.7)–(4.9) are evaluated numerically using a trapezoidal method and $f(r)$ can be a complex quantity. This new estimate of $f(r)$ is used as the shear correction function for the next iteration. As with any smeared laminate model, there are two distinct ways to calculate the shear stress distribution: from the material constitutive relations; or by elemental stress equilibrium. The ultimate goal of the iterative analysis is the determination of the function, $f(r)$, that causes the two stress distributions to be equal. This defines the convergence point for the iterative function $f(r)$, the point at which the stresses and strains are self-consistent.

5. RESULTS AND DISCUSSION

Numerical results were generated to observe the effects of curvature, core thickness and adhesive shear modulus on the system natural frequencies ω_n and modal loss factors η_n. Vaswani *et al.* [20] assembled a series of design curves for the dynamic characterization of a three-layer damped circular ring segment which is simply supported at each end, (see Figure 1). The model assumes that all transverse shear deformation and energy dissipation occurs in the core material. The dissipation is modelled using a complex modulus formulation. The resonant frequencies and the associated system loss factor have been experimentally determined for four sandwich beam specimens and the values compared with those obtained theoretically. Reasonably good agreement is seen between the

theoretical and experimental results. However, the model of Vaswani *et al.* overpredicts natural frequencies by 5%, approximately. The present smeared laminate model was compared to design curves a reference [20] for the first four transverse modes with simply-supported boundary conditions.

The adhesive shear modulus plays a very important role in the damping of the sandwich circular ring segments. The variations of the lowest natural frequency and associated loss factor with respect to the shear modulus G_2 (= real part of $\mathbf{G}_2^*$) is given in Table 1 for the three-layer arch using reference [20]'s design curves and the present laminate model. The input data used here were $h_1 = h_2 = h_3 = 2{\cdot}0$ mm, $\vartheta = 1{\cdot}0$, $\alpha_2 = \beta_2 = 0{\cdot}5$, $R = 1{\cdot}0$ m, $E_1 = E_3 = 6{\cdot}88 \times 10^{10}$ N/m^2, $G_1 = G_3 = 2{\cdot}75 \times 10^{10}$ N/m^2, $\rho_1 = \rho_3 = 2{\cdot}7 \times 10^3$ kg/m^3, $\rho_2 = \rho_1/2$. G_2 was varied from $6{\cdot}88 \times 10^4$ N/m^2 to $6{\cdot}88 \times 10^8$ N/m^2 and $E_2 = 3{\cdot}0\ G_2$. The present smeared laminate model frequency predictions are generally consistent with the Vaswani *et al.* results. The slight discrepancy is due to facesheet shear and rotary inertia, effects which Vaswani *et al.* did not consider. Vaswani *et al.* overpredict natural frequencies by 5%, approximately. The modal loss factors predicted by the present laminate model are also in good agreement with those of Vaswani *et al.* The variation of the system loss factor η with the shear modulus G_2 is similar to that obtained for straight sandwich beams. For each core thickness, a maximum is observed which increases as the core thickness increases and is also seen to occur at higher values of the shear modulus. At low values of shear modulus, although the deformations are large, the shear stiffness is small, hence low damping is observed. At very high values of shear modulus, the shear stiffness is high, the deformations are small, again resulting in low damping.

The effects of the adhesive thickness $2h_2$ on the system natural frequencies and loss factors are also studied. The input data in this case were $h_1 = h_3 = 2{\cdot}0$ mm, $\vartheta = 1{\cdot}0$, $\alpha_2 = \beta_2 = 0{\cdot}5$, $R = 1{\cdot}0$ m, $E_1 = E_3 = 6{\cdot}88 \times 10^{10}$ N/m^2, $G_1 = G_3 = 2{\cdot}75 \times 10^{10}$ N/m^2, $\rho_1 = \rho_3 = 2{\cdot}7 \times 10^3$ kg/m^3, $\rho_2 = \rho_1/2$, $G_2 = 6{\cdot}88 \times 10^4$ N/m^2, $E_2 = 3{\cdot}0\,G_2$. The thickness $2h_2$ was increased from 1.0 mm to 5.0 mm in steps of 1.0 mm. The variations of f and η with $2h_2$ are given in Table 2. It can be seen from this table that both f and η increase with $2h_2$.

The third parameter which affects the system natural frequencies and modal loss factors is the radius of curvature R of the middle surface of the adhesive layer. In this case , the angle ϑ is kept constant, while changing R. This means the total length of the sandwich arch system will change with R. The variations of f and η with R are shown in Table 3. The input data was $h_1 = h_2 = h_3 = 2{\cdot}0$ mm, $\vartheta = 1{\cdot}0$, $\alpha_2 = \beta_2 = 0{\cdot}5$, $E_1 = E_3 = 6{\cdot}88 \times 10^{10}$ N/m^2, $G_1 = G_3 = 2{\cdot}75 \times 10^{10}$ N/m^2, $\rho_1 = \rho_3 = 2{\cdot}7 \times 10^3$ kg/m^3, $\rho_2 = \rho_1/2$, $G_2 = 6{\cdot}88 \times 10^4$ N/m^2, $E_2 = 3{\cdot}0G_2$. R was varied from 800 mm to 1200 mm in steps of 100 mm. It can be seen that f decreases with R. The variations of f with R are obvious, as the total length of curved sandwich beam system increases with an increases in R.

TABLE 1

Variation of the lowest frequency and the loss factor with adhesive shear modulus

	20		Present theory	
G_2 (N/m^2)	f (Hz)	η	f (Hz)	η
$6{\cdot}88 \times 10^4$	7·898	0·0644	7·52	0·0644
$6{\cdot}88 \times 10^5$	11·36	0·2504	10·83	0·2504
$6{\cdot}88 \times 10^6$	20·94	0·1696	19·95	0·1696
$6{\cdot}88 \times 10^7$	25·8	0·0272	24·58	0·0273
$6{\cdot}88 \times 10^8$	26·47	0·0029	25·23	0·0034

TABLE 2

Variation of the lowest frequency and the loss factor with adhesive thickness

	20		Present theory	
$2h_2$ (mm)	f (Hz)	η	f (Hz)	η
1·0	17·981	0·0546	17·06	0·0546
2·0	19·1	0·01	18·2	0·01
3·0	20·09	0·138	19·14	0·138
4·0	20·94	0·1696	19·95	0·1696
5·0	21·66	0·196	20·64	0·196

TABLE 3

Variation of the lowest frequency and the loss factor with radius R

	20		Present theory	
R (mm)	f (Hz)	η	f (Hz)	η
800	29·75	0·211	28·35	0·211
900	24·78	0·1895	23·61	0·1895
1000	20·94	0·1696	19·95	0·1696
1100	17·9	0·1516	17·06	0·1516
1200	15·469	0·1357	14·739	0·1357

TABLE 4

Geometrical parameters of the specimens

Specimen	Length (mm)	Radius (mm)	$2h_1$ (mm)	$2h_2$ (mm)	$2h_3$ (mm)
1	900	900	3·12	4·0	3·12
2	300	300	0·66	2·0	0·66
3	300	300	1·5	2·0	0·5

The present smeared laminate model was compared to the Vaswani *et al.* design curves for the first, second, third and fourth modes presented in the pages of Vaswani *et al.* with simply-supported boundary conditions. The geometrical parameters of the specimens are given in Table 4. The input data in this case were $\alpha_2 = \beta_2 = 0{\cdot}5$, $E_1 = E_3 = 6{\cdot}88 \times 10^{10}\ \mathrm{N/m^2}$, $G_1 = G_3 = 2{\cdot}75 \times 10^{10}\ \mathrm{N/m^2}$, $\rho_1 = \rho_3 = 2{\cdot}7 \times 10^3\ \mathrm{kg/m^3}$, $\rho_2 = \rho_1/2$, $G_2 = 6{\cdot}88 \times 10^4\ \mathrm{N/m^2}$, $E_2 = 3{\cdot}0G_2$. The variations of f_n and η_n $(n = 1, 2, 3, 4)$ is given in Table 5 for the three specimens. Reasonably good agreement is seen between the present laminate model and Vaswani *et al.* result.

6. CONCLUSIONS

A new iterative laminate model has been presented for thin sandwich arches that can accurately determine the dynamic stress distribution in soft as well as hard-cored sandwich

TABLE 5

Comparison of frequency and loss factor with results from reference [20] *for a circular ring segment*

	[20]		Present theory	
	f (Hz)	η	f (Hz)	η
First mode				
Specimen 1	22·7	0·1708	21·82	0·1708
Specimen 2	63·24	0·177	60·26	0·177
Specimen 3	68·33	0·1728	65·8	0·1736
Second mode				
Specimen 1	67·54	0·284	66·85	0·284
Specimen 2	185·44	0·3244	183·12	0·3244
Specimen 3	208·37	0·268	207·76	0·2667
Third mode				
Specimen 1	119·5	0·284	118·94	0·2839
Fourth mode				
Specimen 1	181·5	0·248	181	0·2479

archs. This represents an advance over previous smeared laminate models, in which accurate estimates of the stress field were only possible if the assumed displacement field was a reasonable approximation of the actual diplacement field.

REFERENCES

1. P. CHIDAMPARAM and A. W. LEISSA 1993 *Applied Mechnics Review* **46**, 467–483. Vibrations of planar curved beams, rings, and arches.
2. P. A. A. LAURA and M. J. MAURIZI 1987 *The Shock and Vibration Digest* **19**, 6–9. Recent research on vibrations of arch-type structures.
3. S. MARKUS and T. NANASI 1981 *The Shock and Vibrations Digest* **7**, 3–14. Vibrations of curved beams.
4. R. DAVIS, R. D. HENSHELL and G. B. WARBURTON 1972 *Journal of Sound and Vibration* **25**, 561–576. Constant curvature beam finite elements for in-plane vibration.
5. K. M. AHMED 1971 *Journal of Sound and Vibration* **18**, 61–74. Free vibrations of curved sandwich beams by the method of finite elements.
6. K. M. AHMED 1972 *Journal of Sound and Vibration* **21**, 263–276. Dynamic analysis of sandwich beams.
7. R. A. DI. TARANTO 1973 *Journal of Acoustical Society of America* **53**, 748–757. Free and forced response of a laminated ring.
8. Y. P. LU and B. E. DOUGLAS 1974 *Journal of Sound and Vibration* **32**, 513–516. On the forced vibrations of three-layer damped sandwich ring.
9. M. J. SAGARTZ 1977 *Journal of Applied Mechanics* **44**, 299–304. Transient response of three-layered rings.
10. A. TATEMICHI, A. OKAZAKI and M. HIKAYAMA 1980 *Bulletin of Nagaya Institute* **29**, 309–317. Damping properties of curved sandwich beams with viscoelastic layer.
11. F. C. NELSON and D. F. SULLIVAN 1977 *Journal of American Society of Mechanical Engineers* **154**, 1–8. The forced vibrations of a three-layer damped circular ring.
12. O. K. ISVAN, F. C. NELSON 1982 *Mécanique Materiaux Electricité* **394–395**, 447–449. Free vibrations of a three-layer damped circular ring segment.
13. B. KOVACS 1996 *Publications of the University of Miskolc* **36**, 65–76. Free vibrations of a layered damped arch.

14. C. LIAO and J. N. REDDY 1990 *Computers and Structures* **34**, 805–815. Analysis of anisotropic, stiffened composite laminates using a continuum-based shell element.
15. A. BHIMARADDI, A. J. CARR and P. J. MOSS 1989 *Computers and Structures* **31**, 309–317. Generalized finite element analysis of laminated curved beams with constant curvature.
16. M. S. QATU 1992 *Journal of Sound and Vibration* **159**, 327–338. In-plane vibration of slightly curved laminated composite beams.
17. M. S. QATU and A. A. ELSHARKAWY 1993 *Computers and Structures* **47**, 305–311. Vibration of laminated composite arches with deep curvature and arbitrary boundaries.
18. M. S. QATU 1992 *International Journal of Solid and Structures* **30**, 2743–2756. Equations for the analysis of thin and moderately thick laminated composite curved beams.
19. V. YILDIRIM 1999 *Journal of Sound and Vibration* **224**, 575–589. Rotary inertia, axial and shear deformation effects on the in-plane natural frequencies of symmetric cross-ply lami-nated circular arches.
20. J. VASWANI, N. T. ASNANI and B. C. NAKRA 1988 *Composite Sturctures* **10**, 231–245. Vibration and damping analysis of curved sandwich beams with a viscoelastic core.
21. S. HE and M. D. RAO 1992 *Journal of Sound and Vibration* **159**, 101–113. Prediction of loss factors of curved sandwich beams.
22. J. A. ZAPFE and G. A. LESIEUTRE 1997 *Journal ofthe Sound and Vibration* **199**, 275–284. Vibration analysis of laminated beams using an iterative smeared laminate model.
23. B. KOVACS, F. J. SZABO and A. DOBROCZONI 1993 *MicroCAD-SYSTEM '93 International Computer Science Meeting Proceedings, Miskolc, Hungary*, 65–77. Free vibrations of a layered circular ring segment.
24. B. KOVACS 1992 *Ph.D. Thesis, University of Miskolc, Miskolc, Hungary*. Vibration and stability of layered circular arch.
25. J. N. ROSSETTOS 1971 *American Institute of Aeronautics and Astronautics Journal* **9**, 2273–2275. Vibration of slightly curved beams of transversely isotropic composite materials.
26. J. N. ROSSETTOS and D. C. SQUIRES 1973 *Journal of Applied Mechanics* **40**, 1029–1033. Modes and frequencies of transversely isotropic slightly curved Timoshenko beams.
27. A. A. KHDEIR, J. N. REDDY 1997 *International Journal of Solids and Structures* **34**, 1217–1234. Free and forced vibration of cross-ply laminated composite shallow arches.
28. V. YILDIRIM 1999 *Journal of the Mechanical Behavior of Materials* **10**, 165–186. Out-of-plane free vibration characteristics of symmetric cross-ply laminated composite arches with deep curvature.

APPENDIX: EQUATION DEFINITIONS

Equations (2.6)–(2.8) in the main text contain certain A_{ij} and D_{ij} terms which are defined as follows:

$$A_{11} = K_5 + K_2/R^2 - 2K_1/R, \quad A_{12} = 2K_5 - 2K_1/R, \quad A_{13} = -K_2/R^2 + K_1/R,$$

$$A_{14} = K_4 - K_3/R, \quad A_{15} = K_1/R, \quad A_{16} = K_4, \quad A_{17} = K_5, \quad A_{21} = -K_4 + K_3/R,$$

$$A_{22} = -K_4, \quad A_{23} = -K_3/R, \quad A_{24} = -K_6, \quad A_{25} = K_7, \quad A_{31} = K_2/R^2 - K_1/R,$$

$$A_{32} = -K_1/R, \quad A_{33} = -K_2/R^2, \quad A_{34} = -K_3/R,$$

$$D_{11} = M_1 - 2M_2/R + M_3/R^2, \quad D_{12} = M_2/R - M_3/R^2, \quad D_{13} = M_4 - M_5/R,$$

$$D_{14} = -M_1, \quad D_{21} = -M_4 + M_5/R, \quad D_{22} = -M_5/R, \quad D_{23} = -M_6,$$

$$D_{31} = -M_2/R + M_3/R^2, \quad D_{32} = \text{-}M^3/\mathrm{R}^2, D_{33} = -M_5/R.$$

Equation (3.5) in the main text contain K_{ij} and M_{ij} terms which are defined as follows:

$$K_{11} = k_n^2 K_2/R^2, \quad K_{12} = K_{21} = -k_n K_1/R + k_n^3(K_1/R - K_2/R^2),$$

$$K_{13} = K_{31} = k_n^2 K_3/R, \quad K_{22} = (2k_n^2 - 2k_n^4)K_1/R + k_n^4 K_2/R^2 + (1 - 2k_n^2 + k_n^4)K_5,$$

$$K_{23} = K_{32} = -k_n K_4 + k_n^3(K_4 - K_3/R), \quad K_{33} = K_7 + k_n^2 K_6,$$

$$M_{11} = -M_3/R^2, \quad M_{12} = M_{21} = k_n(M_2/R - M_3/R^2),$$

$$M_{13} = M_{31} = M_5/R, \quad M_{22} = M_1 + k_n^2(M_1 - 2M_2/R + M_3/R^2),$$

$$M_{32} = M_{23} = k_n(M_4 - M_5/R), \quad M_{33} = M_6.$$

APPENDIX B: NOMENCLATURE

b	width of the arch
E_i	elastic modulus of layer i
$\mathbf{E}_2^*$	complex modulus in tension
$\mathbf{e}_r$	unit vector in the radial direction
$\mathbf{e}_\varphi$	unit vector in the transverse direction
$\mathbf{e}_z$	unit vector in the z-direction
$\varepsilon_{\varphi i}$	tensile strain of layer i
$f(r)$	shear correction function
$\gamma_{r\varphi i}$	shear strain of layer i
$\mathbf{G}_2^*$	complex modulus in shear
G_i	shear modulus of layer i
h_i	half-thickness of layer i
φ	circumferential co-ordinate
n	mode number
r	cylindrical co-ordinate
R	radius of centreline of the arch
T	kinetic energy
$\sigma_{\varphi i}$	tensile stress of layer i
$\tau_{r\varphi i}$	shear stress of layer i
$\mathbf{t}_i$	displacement vector of layer i
R_1	radius at the bottom of the first layer
R_2	radius at the top of the first layer
R_3	radius at the bottom of the third layer
R_4	radius at the top of the third layer
α_2	material loss factor in tension of the second layer
β_2	material loss factor in shear of the second layer
η_n	composite loss factor for the nth mode
ω_n	frequency of oscillation in radians for the nth mode
f_n	frequency of oscillation in Hertz for the nth mode
ρ_i	density of layer i
ϑ	opening angle of ring segment
v	tangential displacement of the centreline
w	radial displacement of the centreline